The 2025 World Congress on
Advances in Structural Engineering and Mechanics (ASEM25)
BEXCO, Busan, Korea, August 11-14, 2025

Characterizing effective supplemental damping properties for seismic evaluation of asymmetrical buildings with viscous dampers

*Jui-Liang Lin[1)]

[1)] *National Center for Research on Earthquake Engineering, Taiwan, R.O.C.*
[1)] jllin@niar.org.tw

ABSTRACT

Building codes stipulate that design response spectra can be reduced when the damping ratio of the concerned building exceeds 5%. To reduce the 5%-damped design response spectrum, it is necessary to quantify the effective damping of non-proportionally damped buildings. It is recognized that not only the resultant damping but also the distribution characteristic of viscous dampers across the floors of a building affects the seismic response of asymmetric-plan buildings. For this reason, this study proposes a method to characterize the effective damping properties of non-proportionally damped two-way asymmetric-plan buildings. The proposed method involves constructing a non-proportionally damped three-degree-of-freedom (3DOF) oscillator in modal space. This modal oscillator reflects the characteristic of the dominant mode in each of the three directions of the two-way asymmetric-plan building. By mapping the seismic response of the 3DOF oscillator into physical space, the seismic response of a 20-story example building was satisfactorily estimated.

1. INTRODUCTION

Damping reduction factors are utilized to adjust the 5%-damped design response spectra stipulated by building codes when incorporating supplemental damping into buildings (FEMA-356, 2000; ASCE/SEI 41-13, 2014). Numerous research works have endeavored to propose new methods or compare different methods for computing damping reduction factors (Lin et al., 2005; Cardone et al., 2009; Cameron & Green, 2007; Zhou et al., 2014). Before applying damping reduction factors to adjust 5%-damped design response spectra, it is crucial to determine the level of damping that can be achieved with added dampers. Charney and McNamara (2008) compared three methods, including modal strain energy using undamped mode shapes, free vibration log decrement, and complex eigenvalue-eigenvector analysis, for computing equivalent viscous damping ratios of structures with added viscous dampers. They concluded that the three analysis methods resulted in significantly different values of equivalent viscous damping ratios. In order to consider the combined effect of shear and flexural deformation

[1)] Professor

of buildings, Hwang et al. (2008) proposed new design formulas showing the relationship between the damping coefficients of added viscous dampers and the equivalent damping ratio. In the proposed design formulas, the axial deformation of a damper was computed by considering both the vertical and horizontal deformations between the ends of the damper.

ASCE/SEI 41-13 (2014) stipulates the computation of effective damping (denoted as β_{eff}) resulting from linear viscous dampers as follows:

$$\beta_{eff} = \beta_0 + \beta_{sd} = \beta_0 + \frac{T\sum_j C_j \cos^2\theta_j \phi_{rj}^2}{4\pi\sum_i \left(\frac{w_i}{g}\right)\phi_i^2} \tag{1}$$

where β_0 is the inherent damping of the building and β_{sd} is the supplemental damping, T is the fundamental period of the building, θ_j is the angle of inclination of device j to the horizontal, ϕ_{rj} is the first mode relative displacement between the ends of device j in the horizontal direction, w_i is the reactive weight of floor level i, and ϕ_i is the first mode displacement at floor level i. Given the effective damping β_{eff} (Eq. 1), modal response spectrum analysis or modal response history analysis can be conducted. Due to non-proportional or non-classical damping, seismic responses between vibration modes are usually coupled. Therefore, real-valued modal response spectrum analyses are simply an approximate approach for analyzing non-proportionally damped buildings (Lin et al., 2015). Moreover, supplemental damping in buildings generally results in different effective damping ratios for different vibration modes. Therefore, conducting modal response spectrum analyses with an identical supplemental damping ratio applied to reduce spectral values across all spectral periods is questionable.

It is common practice to symmetrically install viscous dampers in a symmetrical building. In such a case, the only supplemental damping property that needs quantification is the supplemental damping β_{sd}. When placing viscous dampers in an asymmetric-plan building, it is necessary to consider not only the resultant damping but also the distribution characteristic of added viscous dampers across floor plans. Goel (2000) noted that in addition to the effective supplemental damping ratio (denoted as ξ_{sd}), effective supplemental damping eccentricity (denoted as e_{sd}) and effective supplemental damping radius of gyration (denoted as ρ_{sd}) are the properties collectively characterizing the resultant effect of supplemental damping on the seismic response of a one-way asymmetric-plan building.

Lin (2017) further developed the EOSB for proportionally damped two-way asymmetric-plan buildings. This EOSB, which was a 3DOF oscillator in modal space, constituted the 3DOF modal properties of the first triplet of vibration modes of the concerned two-way asymmetric-plan building (Lin & Tsai, 2008). These vibration modes include the fundamental mode in each of the three directions, i.e., two translational directions and one rotational direction. The present study aims to develop the non-proportionally damped EOSB for an N-story two-way asymmetric-plan building with linear viscous dampers when the $3N \times 3N$ supplemental damping matrix of the N-story building is not accessible. Once the 3×3 supplemental damping matrix of the EOSB is constructed, the effective supplemental damping properties of the N-story building can be

characterized. The non-proportionally damped EOSB, a 3DOF modal oscillator reflecting the dominant mode in each of the three directions of the building, is then utilized to estimate the seismic response of the *N*-story building (Figure 1).

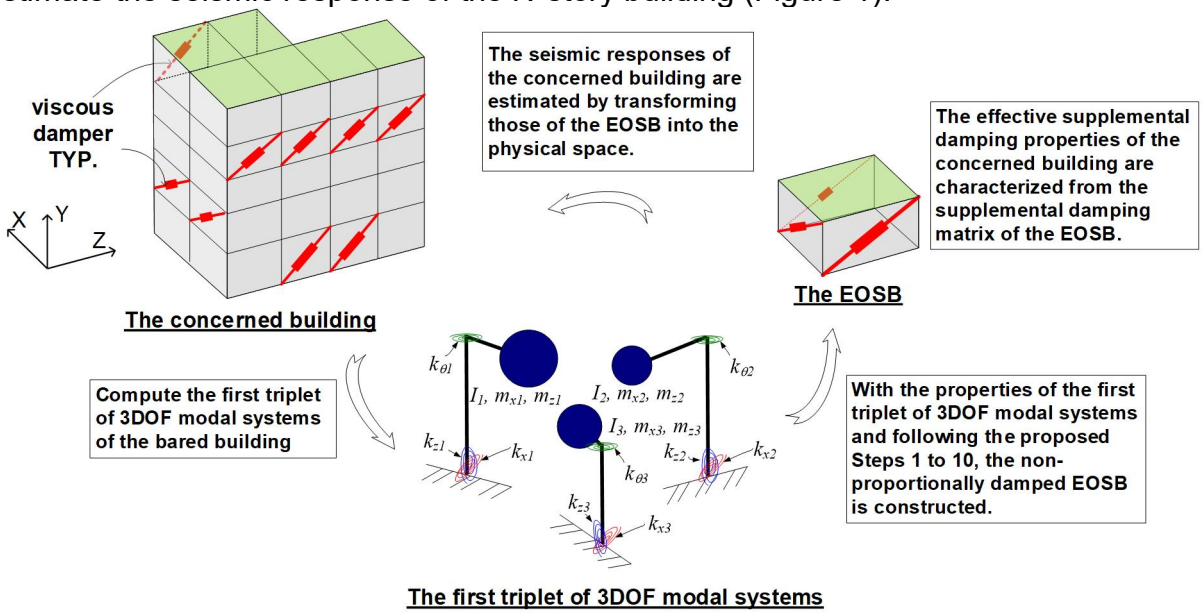

Fig. 1 Schematic diagram of the proposed EOSB for non-proportionally damped two-way asymmetric-plan buildings

2. METHODOLOGY

The EOSB of a proportionally damped *N*-story two-way asymmetric-plan building is available at Lin (2017). The procedures of constructing the supplemental damping matrix of an EOSB for non-proportionally damped two-way asymmetric-plan buildings are as follows:

The damping term of the equation of motion of a non-proportionally damped EOSB consists of two parts: inherent damping (denoted as $\mathbf{C}_0^*$) and supplemental damping (denoted as $\mathbf{C}_{sd}^*$), yielding $\left(\mathbf{C}_0^*+\mathbf{C}_{sd}^*\right)\left[\dot{u}_x^* \quad \mu^*\dot{u}_z^* \quad r^*\dot{u}_\theta^*\right]^T$. The inherent damping is assumed to be Rayleigh damping, with the damping ratios of the EOSB's first two vibration modes equal to those of the first two vibration modes of the first triplet vibration modes of the concerned building without dampers. In other words, $\mathbf{C}_0^*$ can be directly obtained from the mass and stiffness matrices of the EOSB. The supplemental damping $\mathbf{C}_{sd}^*$ is expressed as:

$$\mathbf{C}_{sd}^* = \begin{bmatrix} C_{xx} & 0 & -C_{xx}e_{sdz} \\ 0 & C_{zz} & C_{zz}e_{sdzx} \\ -C_{xx}e_{sdz} & C_{zz}e_{sdzx} & C_{\theta\theta}+C_{xx}e_{sdz}^2+C_{zz}e_{sdx}^2 \end{bmatrix} \tag{1}$$

Five parameters in Eq. 1, including three supplemental damping coefficients (C_{xx}, C_{zz}, and $C_{\theta\theta}$) and two supplemental damping eccentricities (e_{sdx} and e_{sdz}), need to be determined. It would be better that the determination of the values of the five parameters is independent on input ground motions because real ground motions induced by future earthquakes are never known. It is aware that the displacement response of an SDOF oscillator subjected to a unit impulse is the unit impulse-response function. The complete response history of an SDOF oscillator subjected to a ground motion is a composition of unit impulse-response functions (Chopra, 2007). The unit impulse-response function is the inverse Fourier transform of the frequency response function, a general dynamic property of an oscillator independent of the characteristics of input excitations. Utilizing a unit impulse to excite the EOSB, the procedure for determining the values of the five parameters (C_{xx}, C_{zz}, $C_{\theta\theta}$, e_{sdx}, and e_{sdz}) are as follows:

Step 1: The peak x-directional roof displacement (denoted as $u_{xr,peak}$) of the bare building (i.e., the building without dampers) subjected to an x-directional unit impulse (i.e., x-directional ground acceleration with a unit acceleration at a single time point and zero accelerations at other time points) is computed. Similarly, the peak x-directional displacement (denoted as $u^*_{x,peak}$) of the bare EOSB (i.e., the EOSB without supplemental damping matrix $\mathbf{C}^*_{sd}$) subjected to an x-directional unit impulse is computed. The x-directional mapping factor is accordingly obtained as $\eta_x = u_{xr,peak} \big/ u^*_{x,peak}$.

Step 2: This is similar to Step 1, except that the displacement is calculated for an input z-directional unit impulse excitation of the bare building and the bare EOSB. Accordingly, the z-directional mapping factor is obtained as $\eta_z = u_{zr,peak} \big/ u^*_{z,peak}$.

Step 3: The x- and z-directional roof displacement histories (denoted as $u_{xr}(t)$ and $u_{zr}(t)$) of the non-proportionally damped building (i.e., the building with dampers) subjected to x- and z-directional unit impulses are computed, respectively. Similarly, the roof rotational history (denoted as $u_{\theta r}(t)$) of the non-proportionally damped building subjected to a y-rotational unit impulse is computed.

Step 4: From the decaying amplitudes of the displacement histories $u_{xr}(t)$, $u_{zr}(t)$, and $u_{\theta r}(t)$, the initial conjectured values of C_{xx}, C_{zz}, and $C_{\theta\theta}$ (denoted as $C^{(0)}_{xx}$, $C^{(0)}_{zz}$, and $C^{(0)}_{\theta\theta}$) are computed as follows:

$$C^{(0)}_{xx} = 2m_x\omega_x\xi_x = 2m_x\omega_x \frac{\ln\left(\dfrac{u_{xr,1}}{u_{xr,2}}\right)}{2\pi} = \frac{\omega_x}{\pi}\ln\left(\frac{u_{xr,1}}{u_{xr,2}}\right)$$

$$C^{(0)}_{zz} = \frac{\omega_z}{\pi}\ln\left(\frac{u_{zr,1}}{u_{zr,2}}\right), \quad C^{(0)}_{\theta\theta} = \frac{\omega_\theta}{\pi}\ln\left(\frac{u_{\theta r,1}}{u_{\theta r,2}}\right) \tag{2}$$

in which $u_{xr,1}$ and $u_{xr,2}$ represent the first two maximum amplitudes of $u_{xr}(t)$, $u_{zr,1}$ and $u_{zr,2}$ are the first two maximum amplitudes of $u_{zr}(t)$, and $u_{\theta r,1}$ and $u_{\theta r,2}$ represent the first two maximum amplitudes of $u_{\theta r}(t)$. Additionally, ω_x, ω_z, and ω_θ, are the angular

frequencies of the x-translational, z-translational, and y-rotational dominant modes of the EOSB. It is noted that the x-translational, z-translational, and y-rotational dominant modes do not necessarily correspond to the lowest, intermediate, and highest vibration modes of the first triplet of vibration modes of the concerned building.

Step 5: The iteration counter is set to $j = 0$, and the initial conjectured $\mathbf{C}_{sd}^{*}$ is set as follows: $C_{xx} = C_{xx}^{(0)}$, $C_{zz} = C_{zz}^{(0)}$, $C_{\theta\theta} = C_{\theta\theta}^{(0)}$, and $e_{sdx} = e_{sdx}^{(0)} = k_{23}/k_{22}$, $e_{sdz} = e_{sdz}^{(0)} = -k_{13}/k_{11}$, where k_{23}, k_{22}, k_{13}, and k_{11} are the elements of the stiffness matrix of the EOSB (Lin 2017). Because k_{23}/k_{22} and $-k_{13}/k_{11}$ represent the structural eccentricities, the initial conjectured supplemental damping eccentricities ($e_{sdx}^{(0)}$ and $e_{sdz}^{(0)}$) are presumed to be the same as their structural eccentricity counterparts.

Step 6: The three directional roof displacement histories (denoted as $u_{xr}^{b}(t)$, $u_{zr}^{b}(t)$, and $u_{\theta r}^{b}(t)$) of the non-proportionally damped building subjected to a bi-directional unit impulse (i.e., by simultaneously applying unit impulses in x- and z-directions) are computed. The superscript *b* denotes the responses resulting from a bi-directional unit impulse.

Step 7: The iteration counter is set to $j = j + 1$.

Step 8: By varying e_{sdx} and e_{sdz} from $-3e_{sdx}^{(j-1)}$ to $3e_{sdx}^{(j-1)}$ and from $-3e_{sdz}^{(j-1)}$ to $3e_{sdz}^{(j-1)}$, the three directional displacement histories (denoted as $u_{x1}^{*b}(t)$, $u_{z1}^{*b}(t)$, and $u_{\theta 1}^{*b}(t)$) of the non-proportionally damped EOSB subjected to a bi-directional impulse are computed. The bi-directional impulse comprises x-directional and z-directional unit impulses multiplied by η_x and η_z, respectively. The suggested ranges for varying e_{sdx} and e_{sdz} (i.e., from $-3e_{sdx}^{(j-1)}$ to $3e_{sdx}^{(j-1)}$ and from $-3e_{sdz}^{(j-1)}$ to $3e_{sdz}^{(j-1)}$) and their increments can be adjusted depending on a compromise between the required precision and affordable computation time. Of all the considered combinations of e_{sdx} and e_{sdz}, the values of e_{sdx} and e_{sdz} are updated as the pair (denoted as $e_{sdx}^{(j)}$ and $e_{sdz}^{(j)}$) for which the corresponding displacement discrepancy index (denoted as I_{D1}) is minimum, where I_{D1} is computed as:

$$I_{D1}^{(j)} = \frac{1}{3NDP}\sum_{i}^{NDP}\left[\left(u_{x1}^{*b}(t_i) - u_{xr}^{b}(t_i)\right)^2 + \left(u_{z1}^{*b}(t_i) - u_{zr}^{b}(t_i)\right)^2 + \left(au_{\theta 1}^{*b}(t_i) - au_{\theta r}^{b}(t_i)\right)^2\right] \quad (3)$$

NDP represents the number of data points in the response history, and a denotes the width of the building plan. Consequently, $\mathbf{C}_{sd}^{*}$ has been updated by replacing $e_{sdx}^{(j-1)}$ and $e_{sdz}^{(j-1)}$ with $e_{sdx}^{(j)}$ and $e_{sdz}^{(j)}$, respectively.

Step 9: With the updated $\mathbf{C}_{sd}^{*}$ obtained from the previous step and varying C_{xx} from $0.5C_{xx}^{(j-1)}$ to $1.5C_{xx}^{(j-1)}$, C_{zz} from $0.5C_{zz}^{(j-1)}$ to $1.5C_{zz}^{(j-1)}$, and $C_{\theta\theta}$ from $0.5C_{\theta\theta}^{(j-1)}$ to $1.5C_{\theta\theta}^{(j-1)}$, the three directional displacement histories (denoted as $u_{x2}^{*b}(t)$, $u_{z2}^{*b}(t)$,

and $u_{\theta 2}^{*b}(t)$) of the non-proportionally damped EOSB subjected to a bi-directional impulse are computed. The bi-directional impulse consists of x-directional and z-directional unit impulses multiplied by η_x and η_z, respectively. The suggested ranges for varying C_{xx}, C_{zz}, and $C_{\theta\theta}$ (i.e., from $0.5C_{xx}^{(j-1)}$ to $1.5C_{xx}^{(j-1)}$, from $0.5C_{zz}^{(j-1)}$ to $1.5C_{zz}^{(j-1)}$, and from $0.5C_{\theta\theta}^{(j-1)}$ to $1.5C_{\theta\theta}^{(j-1)}$) and their increments can be adjusted depending on a compromise between the required precision and affordable computation time. Of all the considered combinations of C_{xx}, C_{zz}, and $C_{\theta\theta}$, the values of C_{xx}, C_{zz}, and $C_{\theta\theta}$ are updated as the trio (denoted as $C_{xx}^{(j)}$, $C_{zz}^{(j)}$, and $C_{\theta\theta}^{(j)}$) for which the corresponding displacement discrepancy index (denoted as I_{D2}) is minimum, where I_{D2} is computed as:

$$I_{D2}^{(j)} = \frac{1}{3NDP}\sum_{i}^{NDP}\left[\left(u_{x2}^{*b}(t_i) - u_{xr}^{b}(t_i)\right)^2 + \left(u_{z2}^{*b}(t_i) - u_{zr}^{b}(t_i)\right)^2 + \left(au_{\theta 2}^{*b}(t_i) - au_{\theta r}^{b}(t_i)\right)^2\right] \quad (4)$$

As a result, $\mathbf{C}_{sd}^{*}$ has been updated by replacing $C_{xx}^{(j-1)}$, $C_{zz}^{(j-1)}$, and $C_{\theta\theta}^{(j-1)}$ with $C_{xx}^{(j)}$, $C_{zz}^{(j)}$, and $C_{\theta\theta}^{(j)}$, respectively.

Step 10: If the discrepancy between the values of $I_{D2}^{(j)}$ and $I_{D2}^{(j-1)}$ is not acceptable, the iteration continues with Step 7. Otherwise, the eventual $\mathbf{C}_{sd}^{*}$ is obtained and the iteration is stopped. In other words, the non-proportionally damped EOSB has been constructed.

3. NUMERICAL VALIDATION

The example building is a 20-story steel moment-resisting frame building designated as ASY20. ASY20 is a variation of the proportionally damped symmetrical prototype building used in the SAC steel research project to represent a typical office building situated on stiff soil in Los Angeles (FEMA-355C, 2000).

In addition to adding linear viscous dampers, the alteration included the intended movement of the center of mass (CM) of each floor away from the center of rigidity (CR) to achieve eccentricity ratios of 20% and 10% in the x- and z-directions (Figure 2a). The story mass of the top and bottom stories is 585 kN × s^2/m and 564 kN × s^2/m, respectively. The story mass of the other stories is 551.3 kN × s^2/m. The story mass moment of inertia of the top and bottom stories is 110,485 kN × s^2 × m and 106,541 kN × s^2 × m, and the story mass moment of inertia of the other stories is 104,141 kN × s^2 × m. Each floor is simulated with a rigid diaphragm and a lumped mass located at the center of mass. The seismic force-resisting system consists of perimeter steel moment frames with member sizes shown in the related report (FEMA-355C, 2000). The materials used in the beams and columns are dual A36 Grade 50 steel and A572 Grade 50 steel, respectively. The steel materials, with a Young's modulus of E = 2.0 × 10^5 MPa, were assumed to remain elastic. Rayleigh damping with 2% damping ratios for the first two vibration modes of the first triplet of vibration modes of ASY20 was adopted. The Newmark-β numerical integration method provided by the structural analysis program PISA3D was employed

in the dynamic analyses of the numerical building model (Lin et al., 2009).
The added linear viscous dampers, all with a damping coefficient of 20 kN × s/mm, were arbitrarily distributed on the four sides of the perimeter moment-resisting frame. Figure 2b illustrates that on the x-directional flexible side (i.e., frame 1), viscous dampers were installed on the ground, 1st, 2nd, 4th, 5th, 7th, 10th, 15th, and 19th floors. On the x-directional stiff side (i.e., frame 7), viscous dampers were installed on the 1st, 2nd, 4th, 6th, 7th, 8th, 10th, 11th, 15th, and 16th floors. One viscous damper was installed on every floor of the z-directional flexible side (i.e., frame A). There were no dampers on the z-directional stiff side (i.e., frame F). The ensemble of 20 ground motion records (denoted as LA01–LA20) used in the SAC steel research project, was also used in this numerical validation. The ensemble of ground motion records, scaled to a seismic hazard level of a 475-year return period, comprises ten pairs of bi-directional ground motion records. The first and the second components of each pair (e.g., (LA01, LA02), (LA03, LA04)) were applied in the x- and z-directions, respectively. For instance, LA03 and LA04 were applied in the x- and z-directions, respectively. Additionally, the pair of ground motions LA03 and LA04 is denoted as LA0304.

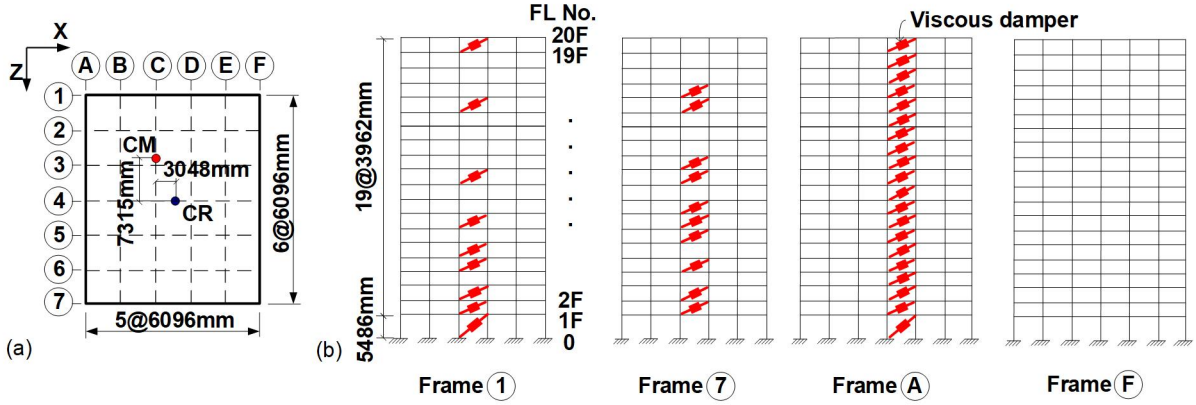

Fig. 2 (a) Typical floor plan and (b) elevations of ASY20

Fig. 3 illustrates the peak story displacements in the three directions along the building height of ASY20 subjected to the first five pairs of ground motions (from LA0102 to LA0910). Fig. 4 is the counterpart of Fig. 3 but is subjected to the other five pairs of ground motions (from LA1112 to LA1920). Generally, the peak story displacements were satisfactorily estimated. It was observed that higher mode effects were more significant as ASY20 was subjected to ground motions LA0102, LA1112, LA1718, and LA1920. Taking the case of ASY20 subjected to ground motion LA0102 as an example, Figures 3a, 3f and 3k indicate that the actual peak displacements along the height of ASY20 do not monotonically increase as the story number increases. Nevertheless, the estimated peak displacements, which were obtained using only the first triplet of vibration modes, cannot reflect this phenomenon.

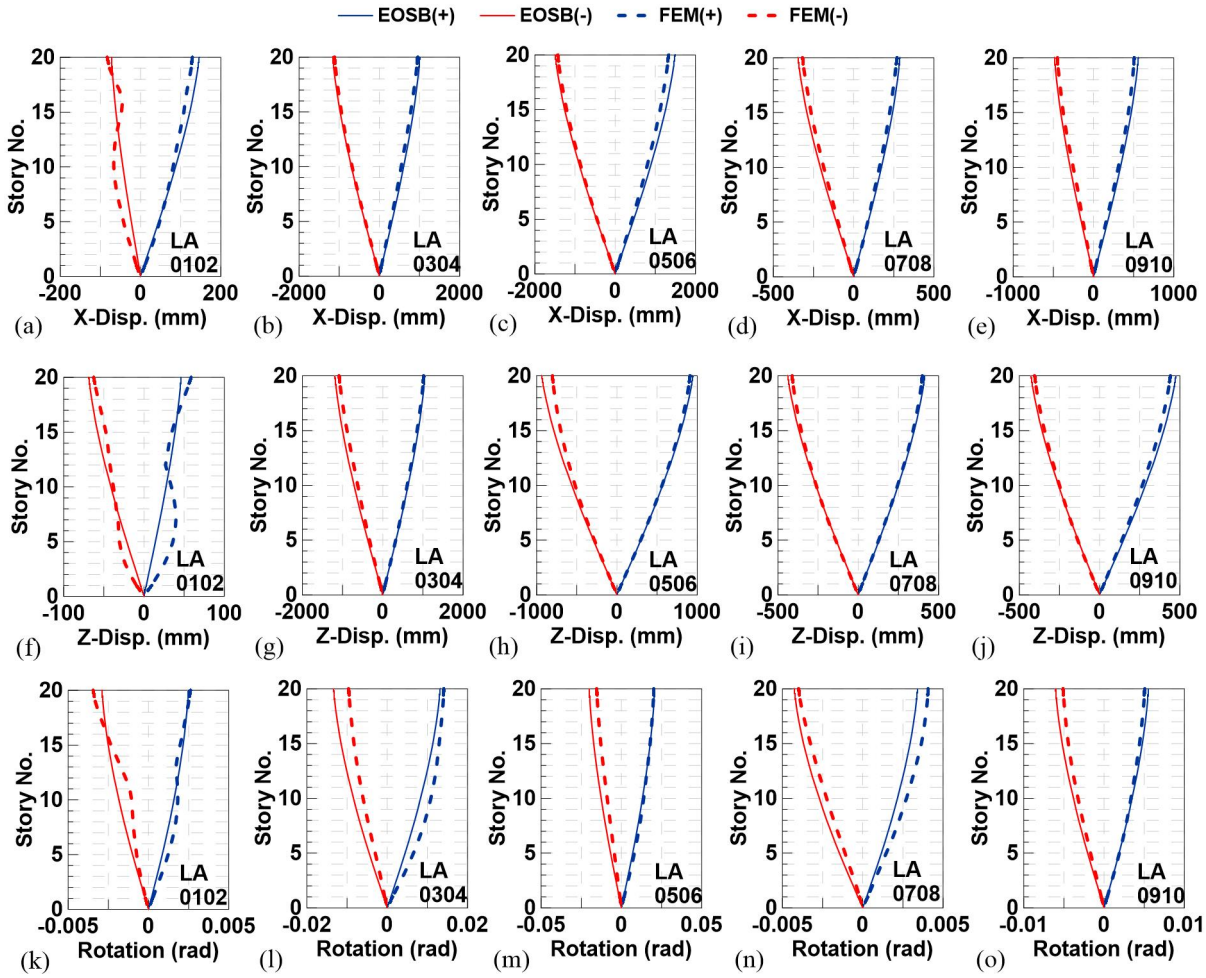

Fig. 3 The x-directional story displacements of ASY20 compared with those estimated from the EOSB while subjected to (a) LA0102, (b) LA0304, (c) LA0506, (d) LA0708, and (e) LA0910 ground motions. Panels (f) to (j) are the counterparts of (a) to (e) but for the z-directional story displacements. Panels (k) to (o) are the counterparts of (a) to (e) but for the y-rotational displacements.

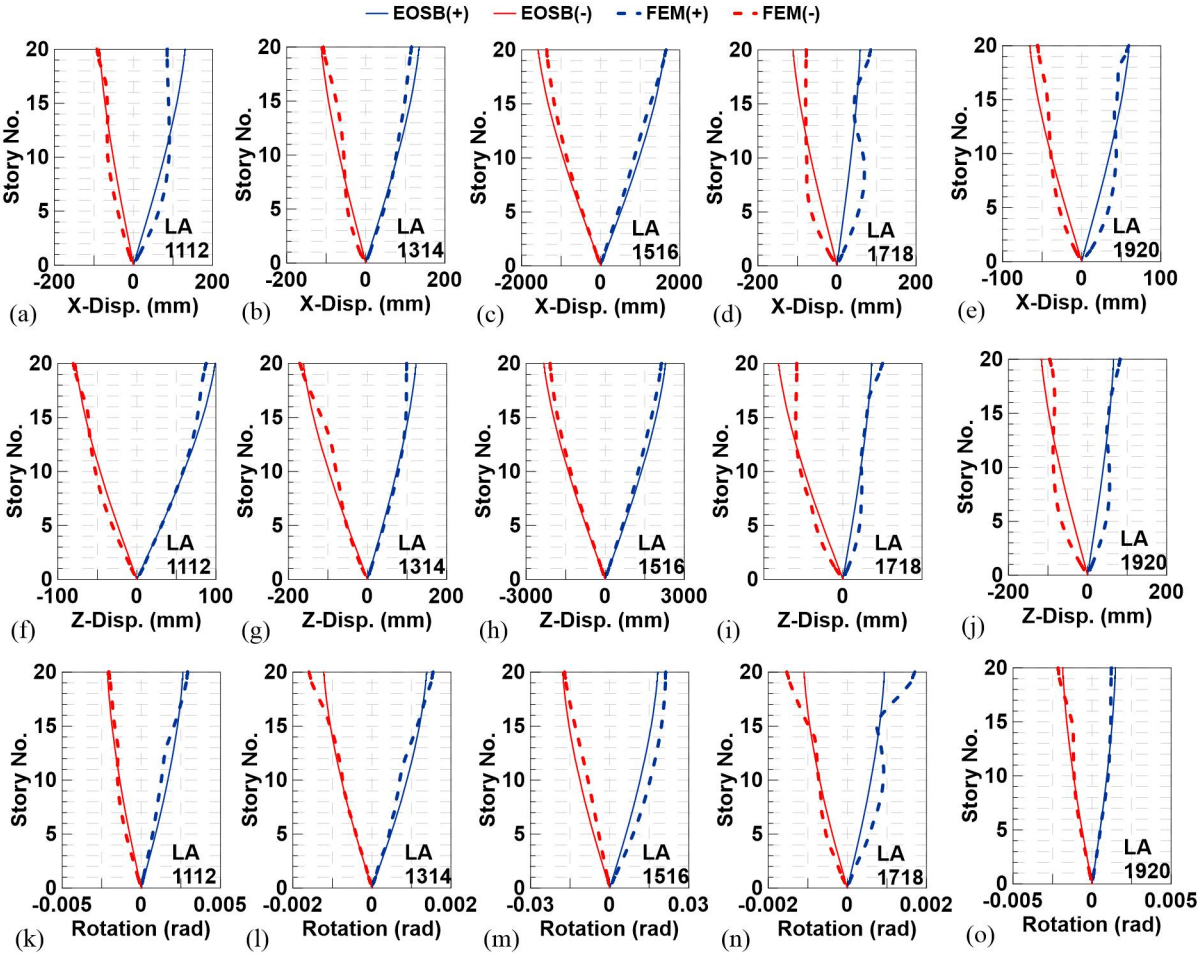

Fig. 4 The x-directional story displacements of ASY20 compared with those estimated from the EOSB while subjected to (a) LA1112, (b) LA1314, (c) LA1516, (d) LA1718, and (e) LA1920 ground motions. Panels (f) to (j) are the counterparts of (a) to (e) but for the z-directional story displacements. Panels (k) to (o) are the counterparts of (a) to (e) but for the y-rotational displacements.

4. CONCLUSIONS

The present study proposed a non-proportionally damped three-degree-of-freedom (3DOF) oscillator as a substitute for a non-proportionally damped two-way asymmetric-plan building in the modal space. The 3DOF oscillator effectively characterizes the resultant supplement damping properties of the fundamental mode in each of the three directions. The displacement demands of a non-proportionally damped 20-story building (designated as ASY20) subjected to ten pairs of bi-directional ground motions were satisfactorily estimated using the proposed 3DOF oscillator. Nevertheless, because the proposed 3DOF oscillator considers only the first dominant modes in the three directions, it is natural that the 3DOF oscillator is not capable of reflecting higher mode effects. The numerical validation using ASY20 clearly shows this issue.

REFERENCES

ASCE (2014), Seismic evaluation and retrofit of existing buildings. ASCE/SEI 41-13. Reston (VA): *American Society of Civil Engineers* (ASCE).

Cameron, W.I., and Green, R.A. (2007), "Damping Correction Factors for Horizontal Ground-Motion Response Spectra", *Bulletin of the Seismological Society of America*, **97**(3), 934-960.

Cardone, D., Dolce, M., and Rivelli, M. (2009), "Evaluation of reduction factors for high-damping design response spectra", *Bulletin of Earthquake Engineering*, **7**, 273-291.

Charney, F.A., and McNamara, R.J. (2008), "Comparison of methods for computing equivalent viscous damping ratios of structures with added viscous damping", *Journal of Structural Engineering*, ASCE, **134**, 32-44.

Chopra, A.K. (2007), Dynamics of Structures: Theory and Applications to Earthquake Engineering, 3rd Edition. Prentice Hall: New Jersey.

FEMA-355C (2000), State of the art report on systems performance of steel moment frames subject to earthquake ground shaking, SAC Joint Venture for the Federal Emergency Management Agency, Washington, DC.

FEMA-356 (2000). Prestandard and commentary for the seismic rehabilitation of buildings. Federal Emergency Management Agency, Washington D.C.

Goel, R.K. (2000), "Seismic behavior of asymmetric buildings with supplemental damping", *Earthquake Engineering and Structural Dynamics*, **29**, 461-480.

Hwang, J.S., Huang, Y.N., Yi, S.L., and Ho, S.Y. (2008), "Design formulations for supplemental viscous dampers to building structures", *Journal of Structural Engineering*, ASCE, **134**, 22-31.

Lin, B.Z., Chuang, M.C., and Tsai, K.C. (2009), "Object-oriented development and application of a nonlinear structural analysis framework", *Adv Eng Softw*, **40**, 66-82.

Lin, J.L., Liu, T.H. and Tsai, K.C. (2015), "Real-valued modal response history analysis for asymmetric-plan buildings with nonlinear viscous dampers", *Soil Dynamics and Earthquake Engineering*, **77**, 97-110.

Lin, J.L. (2017), "Top-story mass dampers for seismic control of the first triplet of vibration modes of two-way asymmetric-plan buildings", *Journal of Vibration and Control*, **23** (18), 2962-2976.

Lin, J.L. and Tsai, K.C. (2008), "Seismic analysis of two-way asymmetric building systems under bi-directional seismic ground motions", *Earthquake Engineering and Structural Dynamics*, **37**, 305-328.

Lin, Y.Y., Miranda, E., and Chang, K.C. (2005), "Evaluation of damping reduction factors for estimating elastic response of structures with high damping", *Earthquake Engineering and Structural Dynamics*, **34**, 1427-1443.

Zhou, J, Tang, K., Wang, H., and Fang, X. (2014), "Influence of Ground Motion Duration on Damping Reduction Factor", *Journal of Earthquake Engineering*, **18**, 816-830.